Crystal Structures of the Kinase Domain of c-Abl in Complex with the Small Molecule Inhibitors PD173955 and Imatinib (STI-571)

Bhushan Nagar, William G. Bornmann, Patricia Pellicena, et al.

Cancer Res 2002;62:4236-4243.

[CANCER RESEARCH 62, 4236–4243, August 1, 2002]

Crystal Structures of the Kinase Domain of c-Abl in Complex with the Small Molecule Inhibitors PD173955 and Imatinib (STI-571)[1]

Bhushan Nagar, William G. Bornmann, Patricia Pellicena, Thomas Schindler,[2] Darren R. Veach, W. Todd Miller, Bayard Clarkson, and John Kuriyan[3]

Departments of Molecular and Cell Biology and Chemistry and Howard Hughes Medical Institute, University of California, Berkeley, California 94720 [B. N., P. P., J. K.]; Physical Biosciences Division, Lawrence Berkeley National Lab, Berkeley, California 94720 [B. N., P. P., J. K.]; Memorial Sloan-Kettering Cancer Center, New York, New York 10021 [W. G. B., D. R. V., B. C.]; Laboratories of Molecular Biophysics, The Rockefeller University, New York, New York 10021 [T. S.]; and Department of Physiology and Biophysics, School of Medicine, State University of New York at Stony Brook, Stony Brook, New York 11794 [W. T. M.]

ABSTRACT

The inadvertent fusion of the *bcr* gene with the *abl* gene results in a constitutively active tyrosine kinase (Bcr-Abl) that transforms cells and causes chronic myelogenous leukemia. Small molecule inhibitors of Bcr-Abl that bind to the kinase domain can be used to treat chronic myelogenous leukemia. We report crystal structures of the kinase domain of Abl in complex with two such inhibitors, imatinib (also known as STI-571 and Gleevec) and PD173955 (Parke-Davis). Both compounds bind to the canonical ATP-binding site of the kinase domain, but they do so in different ways. As shown previously in a crystal structure of Abl bound to a smaller variant of STI-571, STI-571 captures a specific inactive conformation of the activation loop of Abl in which the loop mimics bound peptide substrate. In contrast, PD173955 binds to a conformation of Abl in which the activation loop resembles that of an active kinase. The structure suggests that PD173955 would be insensitive to whether the conformation of the activation loop corresponds to active kinases or to that seen in the STI-571 complex. *In vitro* kinase assays confirm that this is the case and indicate that PD173955 is at least 10-fold more inhibitory than STI-571. The structures suggest that PD173955 achieves its greater potency over STI-571 by being able to target multiple forms of Abl (active or inactive), whereas STI-571 requires a specific inactive conformation of Abl.

INTRODUCTION

Tyrosine kinases are a family of tightly regulated enzymes, and the aberrant activation of various members of this family is one of the hallmarks of cancer. In CML,[4] the Abelson tyrosine kinase is improperly activated by the accidental fusion of the *bcr* gene with the gene encoding the intracellular non-receptor tyrosine kinase, c-Abl. Wild-type c-Abl is a large (~1150 residue) protein. The NH_2-terminal half (~530 residues) of c-Abl bears 42% sequence identity to the Src family of tyrosine kinases (excluding the NH_2-terminal unique domain) and shares a similar domain organization, containing two modular peptide binding units (the SH2 and SH3 domains) followed by a tyrosine kinase domain. However, c-Abl is distinct from the Src kinases in that it lacks a critical tyrosine residue that follows the kinase domain of c-Src. Phosphorylation of this tyrosine residue results in the inactivation of the Src kinases. The COOH-terminal half of c-Abl contains DNA and actin-binding domains interspersed with sites of phosphorylation and other short recognition motifs, including proline-rich segments and nuclear localization signals (1). Under normal conditions, c-Abl exists in a regulated state with very low kinase activity (2). In CML, however, the fusion of Bcr to the NH_2 terminus of c-Abl results in the constitutive activation of Abl kinase activity by a mechanism that is not well understood. Bcr-Abl phosphorylates cellular proteins extensively and transforms cells, making them growth factor independent (3).

The catalytic domains of eukaryotic Ser/Thr and tyrosine kinases are highly conserved in sequence and structure. The kinase domain has a bilobal structure. The N-lobe contains a β-sheet and one conserved α-helix (helix C). The C-lobe is largely helical. At the interface between the two lobes, a number of highly conserved residues form the ATP-binding pocket and the catalytic machinery. Small molecule inhibitors of protein kinases that have been discovered to date almost invariably bind to the kinase domain at this interfacial cleft between the two lobes, displacing ATP.

Of importance for the development of treatments for CML are a number of small molecule compounds that can inhibit the tyrosine kinase activity of the Bcr-Abl protein with some degree of selectivity. A member of the class of 2-phenylaminopyrimidine compounds, STI-571 (originally called CGP57148B and now known as imatinib, Fig. 1*a*), was identified in 1996 by Novartis and shows promise as a therapeutic agent (4, 5). STI-571 has now been approved by the Food and Drug Administration for treatment of CML.

We have previously reported the crystal structure of the kinase domain of Abl complexed to a variant of STI-571 [AblK:STI-571 (variant)], lacking the piperazinyl group (Fig. 1*a*; Ref. 6). The structure showed that STI-571 specifically recognizes an inactive and unphosphorylated conformation of Abl. An inactive conformation of the Abl kinase domain appears to be crucial to the selectivity of STI-571 because the observed conformation differs from the inactive conformations of other tyrosine kinases, such as the closely related Src kinases, against which STI-571 is inactive. The potency of STI-571 against the activated forms of Bcr-Abl presumably arises from the dynamic nature of kinase molecules, which can switch between inactive and active forms transiently, allowing STI-571 to gain entry.

It has been shown recently that a class of inhibitors based on the pyrido-[2,3-d]pyrimidine core compounds are also active against Abl (7). One such compound (PD173955; Parke-Davis) was shown to block cell proliferation and mitotic progression through inhibition of the Src family of tyrosine kinases (8). In subsequent studies we have shown that PD173955 is effective at shutting down the kinase activity of Bcr-Abl with an IC_{50} of 1–2 nM *in vitro*. Studies with PD173955 on Bcr-Abl-containing cell lines also reveal it to be a highly effective inhibitor, with IC_{50}s ranging from 2 to 35 nM on CML cell lines (see Ref. 9). Like STI-571, PD173955 is also a potent inhibitor of Kit ligand-dependent cell proliferation through inhibition of the receptor tyrosine kinase c-Kit (IC_{50}, ~50 nM). Comparisons with STI-571 reveal that PD173955 is even more effective at shutting down the kinase activity of c-Abl. In contrast to STI-571, PD173955 is also a potent inhibitor of Src kinases (8).

In this study, we report the crystal structure of the kinase domain of c-Abl bound to STI-571 (AblK:STI-571) and confirm that the essen-

Received 4/1/02; accepted 6/24/02.

The costs of publication of this article were defrayed in part by the payment of page charges. This article must therefore be hereby marked *advertisement* in accordance with 18 U.S.C. Section 1734 solely to indicate this fact.

[1] B. N. was supported by a Human Frontier Science Program fellowship. D. V. was supported by Westvaco Corp. and MeadWestvaco Corp. B. C. was supported by National Cancer Institute Grant CA64593.

[2] Present address: F. Hoffmann-La Roche AG, PNRF 93/7.40, CH-4070 Basel, Switzerland.

[3] To whom requests for reprints should be addressed, at Department of Molecular and Cell Biology, 401 Barker MC 3202, University of California, Berkeley, CA 94720. Phone: (510) 643-0137; Fax: (510) 643-2352; E-mail: kuriyan@uclink.berkeley.edu.

[4] The abbreviations used are: CML, chronic myelogenous leukemia; N-lobe, NH_2-terminal lobe; C-lobe, COOH-terminal lobe; PDB, Protein Data Bank; YopH, *Yersinia* protein tyrosine phosphatase; pAbl, phosphorylated Abl; IRK, insulin receptor kinase.

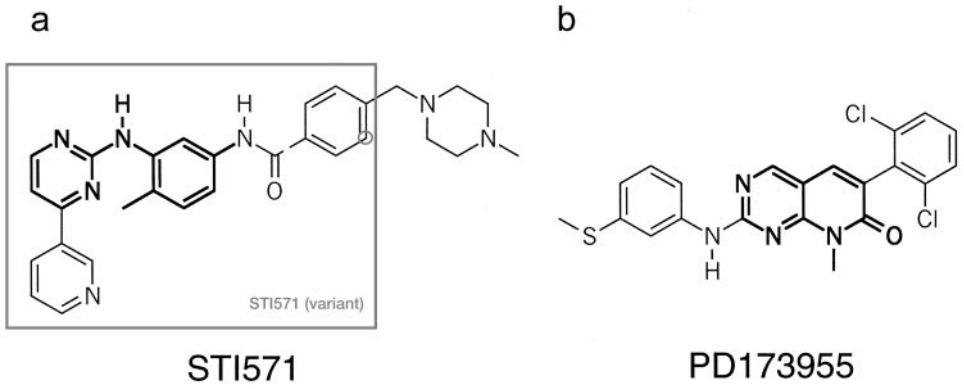

Fig. 1. Chemical structures of (*a*) STI-571 and (*b*) PD173955. The core compounds from which these two inhibitors were developed are shown in *bold lines*. In *a*, a *gray box* outlines the STI-571 variant, and a *gray circle* denotes the position where a carbon atom is replaced by a nitrogen atom in the variant.

tial features of the recognition of the drug by Abl are as inferred earlier from the crystallographic analysis of the smaller STI-571 variant bound to Abl (6). We also present the crystal structure of the Abl kinase domain in complex with PD173955 (AblK:PD173955). This structure reveals that whereas Abl is required to be in a specific inactive conformation to be inhibited by STI-571, PD173955 can probably recognize multiple conformations of the kinase, which is likely to contribute to its greater efficacy as an inhibitor.

MATERIALS AND METHODS

Protein Expression and Purification. The gene encompassing the kinase domain of murine c-Abl (residues 229–515) was cloned into a plasmid in which a His_6 tag is fused to the NH_2 terminus of the protein (pFastbac Hta; Life Technologies, Inc.). Due to a cloning artifact, the construct contains an additional six amino acids (sequence GAMDPS) at the NH_2 terminus. This recombinant plasmid was transformed into *Escherichia coli* (DH10Bac) containing bacmid DNA and helper plasmid. After transposition between donor plasmid and bacmid has taken place (~3–5 h), single colonies containing recombinant plasmid were identified and expanded. Bacmid DNA containing the Abl insert was isolated and transfected into Sf9 insect cells. Baculovirus obtained from the transfection was then used to infect Sf9 cells grown in suspension to a density of 2.5×10^6 cells/ml at a multiplicity of infection of 10. Cells were grown for 48 h and centrifuged, and the pellet stored at −80°C. Cells were thawed, resuspended in buffer A [50 mM Tris-HCl (pH 8.0), 10% glycerol, and 15 mM β-mercaptoethanol] and lysed by sonication. The resulting suspension was diluted (1:2) and centrifuged at 18,000 rpm for 1 h. The supernatant was filtered and loaded onto a 65-ml Q-Sepharose ion-exchange column equilibrated in buffer A. Protein was eluted from the column with a linear salt gradient (0–1 M NaCl). Fractions containing Abl protein (identified by anti-His_6 Western blot) were pooled and loaded onto a Ni-NTA column (Qiagen) equilibrated in 20 mM Tris-HCl (pH 8.0), 500 mM NaCl, 5% glycerol, 20 mM imidazole, and 5 mM β-mercaptoethanol. The protein was eluted with a linear imidazole gradient (20 mM to 1 M). Fractions containing Abl were pooled and incubated with Tobacco Etch Virus protease overnight at 4°C to cleave the His_6 tag from Abl. Next, inhibitor compound (PD173955 or STI-571) dissolved in DMSO was added at 3× the molar protein concentration with constant stirring at 4°C. The inhibitor-protein complex was then concentrated and loaded onto a Sephadex 75 gel filtration column (HiLoad 16/60) equilibrated in 20 mM Tris-HCl (pH 8.0), 100 mM NaCl, and 3 mM DTT. Abl:inhibitor complex-containing fractions were pooled and concentrated to ~10 mg/ml. YopH used for enzymatic analysis was expressed as a glutathione *S*-transferase-fusion protein in *E. coli* and purified on a glutathione *S*-transferase column.

Synthesis of STI-571 and PD173955. STI-571 and PD173955 were synthesized and purified in the Organic Synthesis Core Facility at Memorial Sloan-Kettering Cancer Center as described respectively in Ref. 10 and Ref. 11. The compounds were dissolved as 20 mM aliquots in DMSO and stored at −80°C until needed.

Crystallization and Data Collection. Using the hanging drop vapor diffusion method (1 μl of protein solution + 1 μl of reservoir solution) in a sparse matrix screen, crystals of the AblK:STI-571 complex grew in 25% (w/v) polyethylene glycol 4000, 100 mM MES/NaOH buffer (pH 6.5), and 0.2 M $MgCl_2$ at 4°C (space group F222 with a = 112.9 Å, b = 147.4 Å, and c = 153.4 Å and two molecules in the asymmetric unit), and those of AblK:PD173955 grew in 12% (w/v) polyethylene glycol 20000 and 100 mM MES/NaOH buffer (pH 6.5) at 20°C (space group $P2_12_12$ with a = 115.8 Å, b = 125.7 Å, and c = 56.7 Å and two molecules in the asymmetric unit). Crystals of AblK:PD173955 did grow under other conditions including a condition similar to that used to obtain the AblK:STI-571 crystals, but these crystals were not suitable for diffraction analysis. The crystal form for AblK:STI-571 is similar to that reported previously for the variant of STI-571 (6). The crystals were cryoprotected with the addition of 20% (v/v) ethylene glycol or 20% glycerol (v/v) for AblK:STI-571 and AblK:PD173955, respectively. X-ray diffraction data were collected on crystals flash frozen in liquid propane stored in liquid nitrogen at the Advanced Light Source (beamline 5.0.2) for AblK:PD173955 and CHESS (beamline F1) for AblK:STI-571 (Table 1). All data were integrated and scaled with DENZO and Scalepack (12).

Structure Determination and Refinement. The structure of AblK:STI-571 (PDB entry 1IEP) was solved by computing a difference Fourier electron density map after rigid-body refinement of the previously determined structure (PDB entry 1FPU), from which the inhibitor was removed. The structure of AblK:PD173955 (PDB entry 1M52) was solved by molecular replacement with the program AMoRe (13), using one molecule of Abl (PDB code 1FPU), without inhibitor, as a search model. Both models were subsequently refined with the program CNS (14) using simulated annealing, conjugate gradient least-squares minimization, and individual B-factor refinement with intervening rounds of manual model building using O (15) making extensive use of simulated annealing omit maps (Table 1). With AblK:PD173955, noncrystallographic symmetry restraints were maintained, and only 2 B-factors/residue were applied until the final round of refinement, at which point noncrystallographic symmetry restraints were released, and individual B-factors were refined.

Table 1 *Data collection and refinement statistics*

	AblK:STI571	AblK:PD173955
Diffraction data		
Resolution (Å)	30–2.1 (2.18–2.10)	85–2.60 (2.69–2.60)
Measured reflections (#)	195,316	90,487
Unique reflections (#)	37,004	25,520
Data completeness (%)	99.0 (97.1)	99.0 (99.4)
R_{sym} (%)[a]	4.1 (27.0)	8.2 (36.0)
Refinement		
R-factor/R-free	23.1/26.2	21.1/25.4
Free R test set size (#/%)	2,917/8.2	2,469/9.9
No. of protein atoms	4,458	4,424
No. of heterogen atoms	80	58
No. of solvent atoms	172	140
rmsd[b] bond lengths (Å)	0.005	0.008
rmsd bond angles (°)	1.20	1.40
rmsd B-factors ($Å^2$) (main chain/side chain)	2.27/3.23	2.32/3.93

[a] $R_{sym} = \Sigma \mid I - \langle I \rangle \mid / \Sigma I$, where I is the observed intensity of a reflection, and $\langle I \rangle$ is the average intensity obtained from multiple observations of symmetry-related reflections.

[b] rmsd, root mean squared deviation.

Kinase Assays. A continuous spectrophotometric kinase assay was used to measure the kinase activity of the catalytic domain of Abl. In this assay, ADP that is produced as a result of phosphorylation by the enzyme is coupled to the oxidation of NADH to NAD^+, which produces a decrease in absorbance at 340 nm (16). The assays were carried out in 100 mM Tris-HCl (pH 7.5), 10 mM $MgCl_2$, 0.5 mM ATP, 1 mM phosphoenolpyruvate, 0.28 mM NADH, 89 units/ml pyruvate kinase, 124 units/ml lactate dehydrogenase, 4% DMSO, and 0.5 mM peptide substrate (AEEEIYGEFEAKKKKG) at 30°C in a 150-μl reaction volume. Reactions were initiated by the addition of 10 nM pAbl to the mix containing varying amounts of STI-571 or PD173955. After the activity of pAbl was measured, 0.8 μM YopH was added to measure the effect of the inhibitors on unphosphorylated Abl *in situ*. YopH treatment had no effect on the coupling enzymes in the assay, nor did it significantly change the basal activity of pAbl in the absence of inhibitors. Because our construct showed very inefficient autophosphorylation levels, we used Src to phosphorylate Abl on the activation loop (6, 17, 18) by incubating 1 μM Abl with 50 nM activated c-Src (Life Technologies, Inc.) in buffer containing 100 mM Tris-HCl (pH 7.5), 30 mM $MgCl_2$, and 10 mM ATP for 2 h at 4°C.

RESULTS AND DISCUSSION

Overall Features of the Structures. The three-dimensional structures of the kinase domain of Abl in complex with STI-571 and PD173955 were determined at 2.1 and 2.6 Å, respectively. Both structures are of the unphosphorylated form of Abl. In both crystal forms there are two independent molecules in the crystallographic asymmetric unit. The overall structure of the kinase domain in the two crystal forms is very similar, with the typical bilobal architecture that is conserved among eukaryotic Ser/Thr and tyrosine kinases. Residues 225–350 (mouse c-Abl spliceform I numbering) make up the N-lobe of the kinase, and residues 354–498 comprise the C-lobe. The amino acid sequence of the catalytic domain of murine Abl differs from that of human Abl by one residue, a Ser (mouse) to Asn (human) substitution at position 336, on the surface of the C-lobe.

The Conformation of the Activation Loop Is Very Different in the STI-571 and PD173955 Complexes. There is one region in which the structure of the kinase domain differs markedly between the STI-571 and PD173955 complexes, and this is restricted to the activation loop (residues 381–402 in Abl), a centrally located regulatory element in protein kinases.

Whereas the conformations of protein kinases that are fully active are very similar, there are striking differences in various inactive conformations of kinases from different subfamilies (Fig. 2). These differences include alterations in the interlobe orientation and the disposition of helix αC in the N-lobe. A crucial aspect of the conformational transition between the active and inactive states is the activation loop or segment, which is of varying length and sequence and is often the site of activating phosphorylation in the kinase domain.

In structures of protein kinases that are in a fully active state, the activation loop is in an extended or open conformation (19, 20). There are two crucial aspects to this "active" conformation of the activation loop. First, an aspartic acid residue (Asp-381 in Abl) within a strictly conserved Asp-Phe-Gly (DFG) motif at the NH_2-terminal base of the activation loop is positioned so as to interact properly with a magnesium ion that coordinates the phosphate groups of ATP. Second, the rest of the loop is positioned away from the catalytic center so that the COOH-terminal portion of the activation loop provides a platform for substrate binding.

In the structure of the AblK:STI-571 complex, the conformation of the activation loop is essentially the same as that seen in the previously determined structure of Abl complexed to the STI-571 variant (Ref. 6; Fig. 3*A*, *left*). The NH_2-terminal portion of the activation loop, including the DFG motif, is rotated drastically with respect to the active conformation, so that it is Phe-382 of the DFG motif that points toward the ATP binding site rather than Asp-381. As we discuss below, this altered conformation of Phe-382 is crucial for the proper binding of STI-571. The rest of the activation loop adopts a conformation in which the region surrounding Tyr-393 (the site of activating phosphorylation that is unphosphorylated in this structure) mimics a substrate binding to the enzyme, thereby blocking the active site.

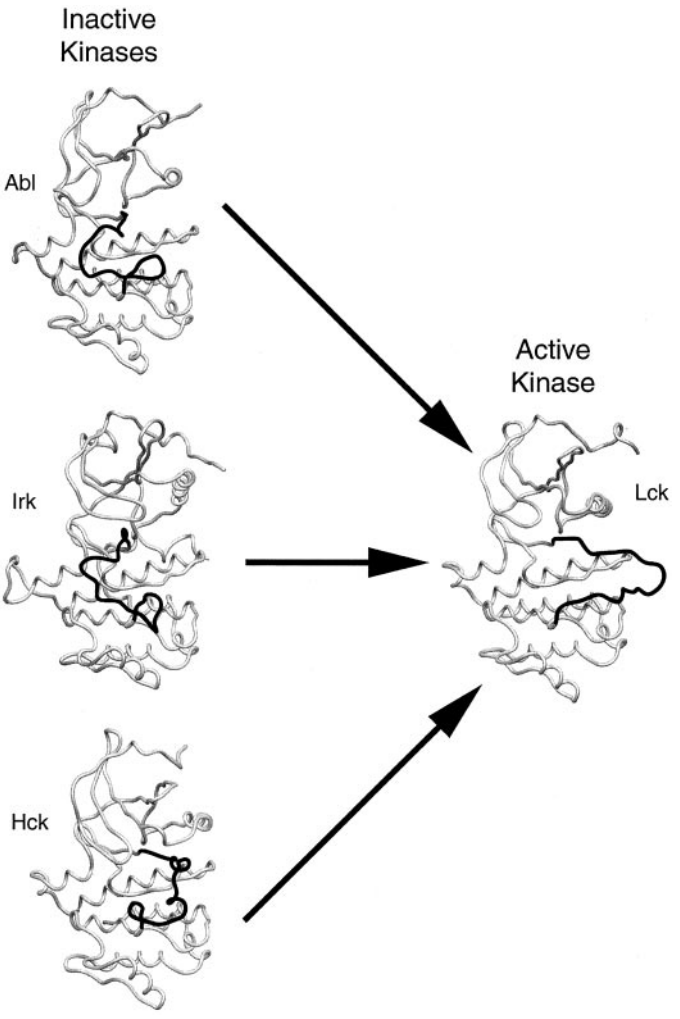

Fig. 2. Conformational changes in the activation loop upon activation of protein kinases. On the *left* are shown three tyrosine kinases (Hck, [PDB code 1QCF; Ref. 24], Irk [1IRK; Ref. 23], and Abl) in inactive states showing distinct conformations of the activation loop (*black*). On the *right* is shown the crystal structure of Lck (3LCK; Ref. 20), which illustrates the conformation of the activation loop (*black*) that all kinases bear upon activation by phosphorylation.

In the AblK:PD173955 complex, most of the activation loop is in a conformation very similar to that seen in active protein kinases, leaving the catalytic center of the enzyme unblocked (Fig. 3*A*, *right*). The conformation of the DFG motif is different from that seen in active kinases (Fig. 4*B*), and it is likely that this is a consequence of the unphosphorylated state of the enzyme. Detailed examination of the structure (see below) indicates that the binding of PD173955 is insensitive to whether the activation loop is in the fully active conformation or not. This is in contrast to STI-571, whose binding to the kinase domain is blocked by the active conformation of the activation loop.

Structure of Abl Kinase Domain Bound to STI-571. STI-571 is derived from a 2-phenylaminopyrimidine scaffold. With reference to the orientation shown in Fig. 1*a*, STI-571 consists of the core scaffold (*bold lines*) plus a pyridine substituent on the bottom left side and a

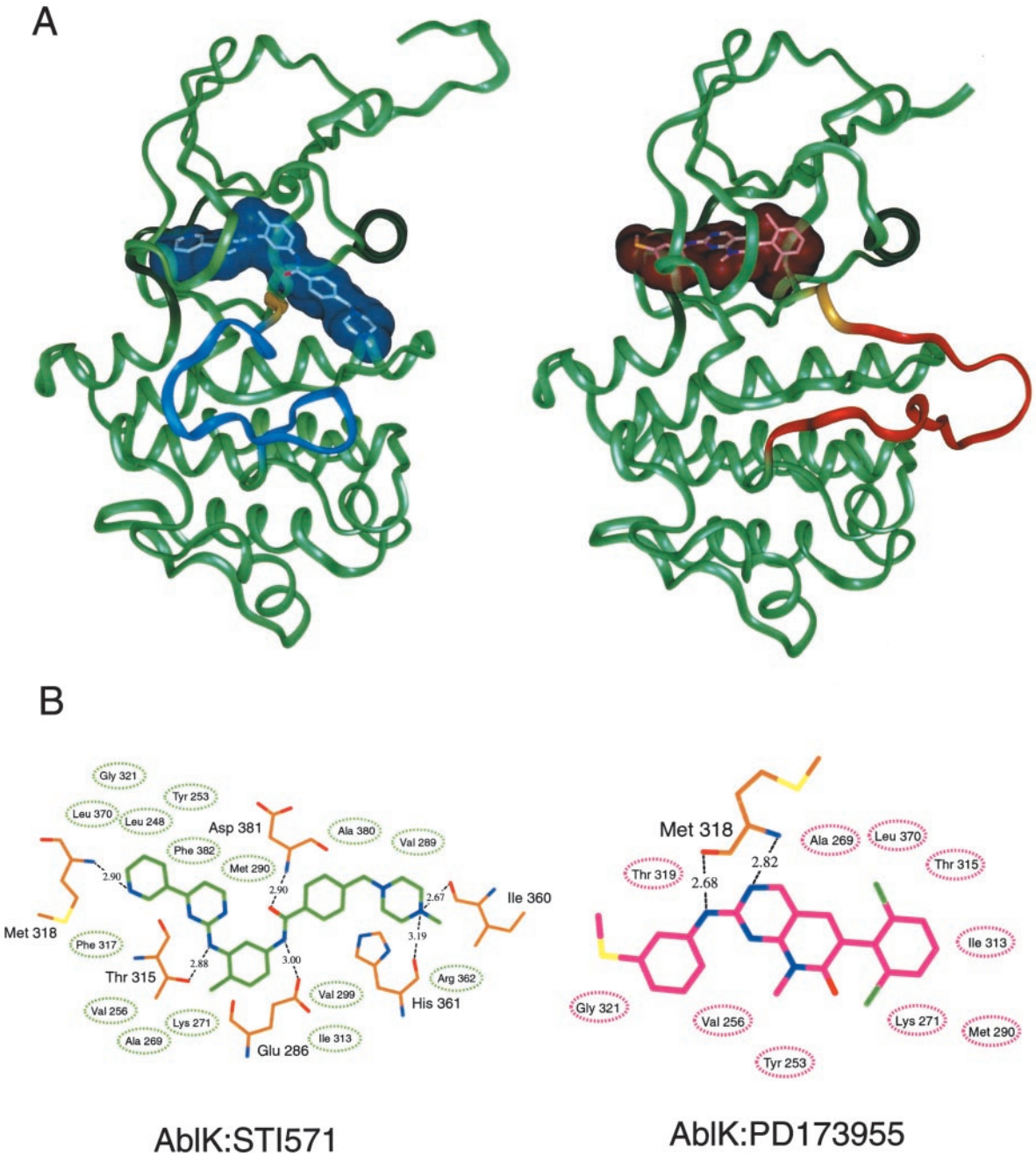

Fig. 3. *A*, ribbon representation of the structure of the Abl kinase domain (*green*) in complex with STI-571 (*left*) and PD173955 (*right*). The activation loops and the van der Waals surfaces corresponding to the inhibitors are colored *blue* and *red* for STI-571 and PD173955, respectively. The DFG motif situated at the NH_2 terminus of the activation loop is colored *gold*. Helix αC and the interlobe connector are colored *dark green*. *B*, schematic diagram of the interactions made by STI-571 (*left*) and PD173955 (*right*) with Abl. Protein residues are labeled and shown in stick representation. Nitrogen atoms are colored *blue*, oxygen atoms are colored *red*, chlorine atoms are colored *green*, sulfur atoms are colored *yellow*, protein carbon atoms are colored *brown*, and inhibitor carbon atoms are colored *green* and *magenta* for STI-571 and PD173955, respectively. Hydrogen bonds are indicated with *dotted lines* along with their distances, and residues making van der Waals interactions with the inhibitor are *circled* with *dotted lines*. Distances were calculated from chain A for AblK:STI-571 and chain B for AblK:PD173955. Additional water-mediated interactions have been omitted.

peptide bond followed by a phenyl ring and a piperazinyl ring to the right of the core. The drug is sandwiched between the N- and C-lobes of the kinase domain and penetrates through the central region of the kinase, from one side to the other (Fig. 3*A*, *left*). Only the leftmost part of STI-571 (pyridine and pyrimidine rings) occludes the region where the adenine ring of ATP normally binds. The rest of the compound penetrates further into the hydrophobic core of the kinase and wedges itself between the activation loop and helix αC, freezing the kinase in an inactive conformation. In total, the compound makes six hydrogen bonds with the protein, and the majority of contacts are mediated by van der Waals interactions (Fig. 3*B*, *left*). A total of 1251 $Å^2$ of surface area is buried between the drug and the protein.

The adenine group of ATP normally makes two hydrogen bonds with backbone atoms of the peptide chain connecting the N- and C-lobes of kinase domains (21). The extracyclic amino group of ATP donates a hydrogen bond to the carbonyl oxygen of the residue corresponding to Glu-316 in Abl, and nitrogen N1 of the purine ring accepts a hydrogen bond from the amide nitrogen of residue Met-318. Many small molecule inhibitors of protein kinases are anchored to the kinase domain by a pair of hydrogen bonds that mimic those formed

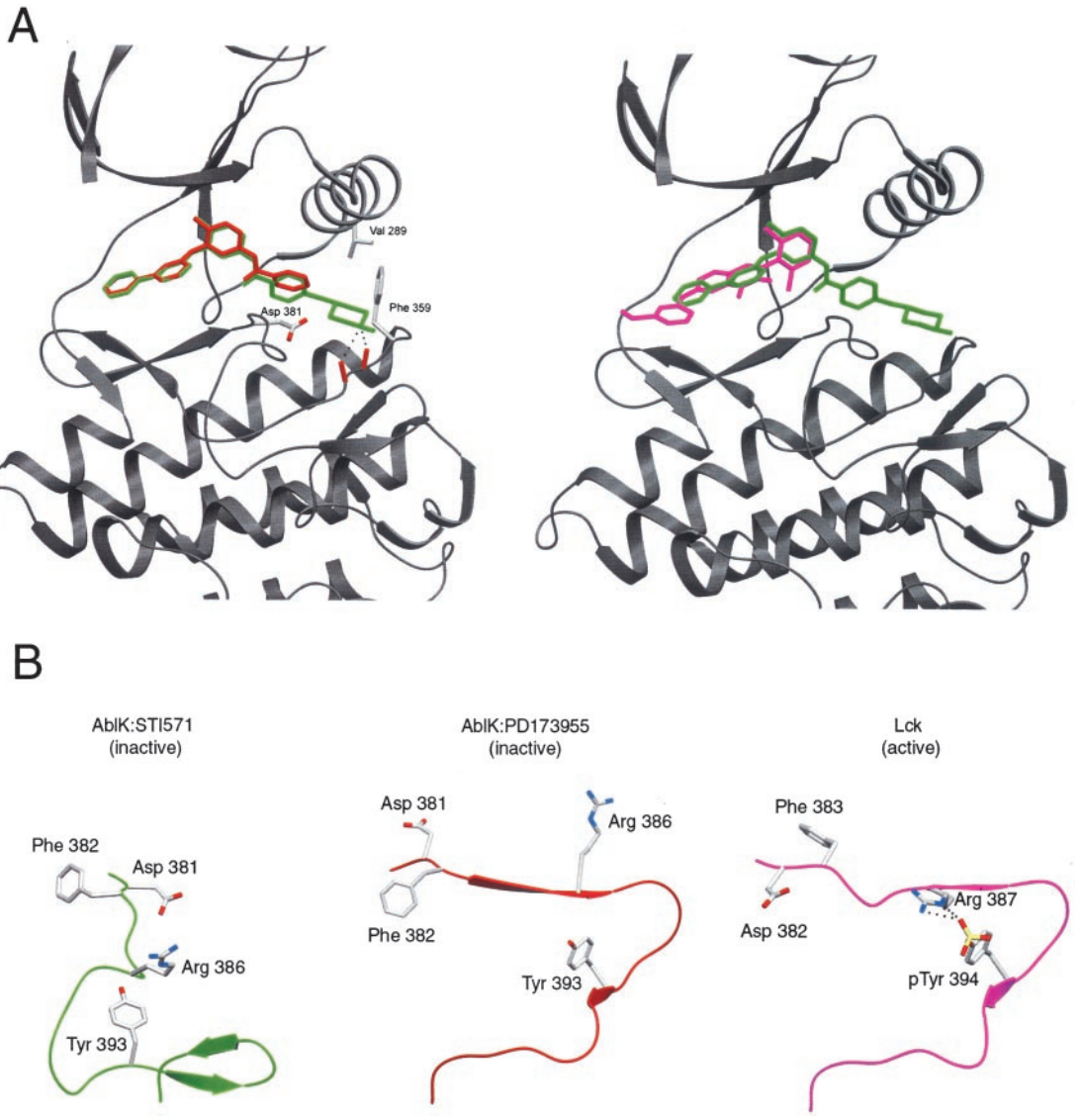

Fig. 4. *A*, Comparison of STI-571 variant (*red*) with STI-571 (*green*) binding to Abl (*left*). Residues whose side chains are shown and labeled are those that make additional van der Waals interactions with the piperazinyl ring of STI-571. Also shown are the two hydrogen bonds (*dotted lines*) made by the carbonyl oxygen atoms (*red*) of Ile-360 and His-361 with the piperazinyl ring. Parts of the protein have been cut away for clarity. Comparison of STI-571 (*green*) and PD173955 (*magenta*) binding to Abl (*right*). *B*, comparison of the activation loops of Abl kinase bound to STI-571 (*green*), Abl kinase bound to PD173955 (*red*), and active Lck (3LCK; Ref. 20; *magenta*). *Dotted lines* indicate salt bridges between the phosphorylated Tyr-394 and Arg-387 in Lck.

by adenine. The pattern of hydrogen bonds formed by STI-571 and the previously analyzed variant (6) are similar, and both lack the hydrogen bond corresponding to that formed by the amino group of adenine to the interlobe connector (a water-mediated hydrogen bond is formed instead). This results in STI-571 being bound more toward the mouth of the kinase domain (that is, displaced away from the interlobe connector) than is typically the case for small molecule inhibitors.

The outward displacement of STI-571 appears to be facilitated by the formation of a hydrophobic cage around the pyridine and pyrimidine ring systems of the drug. This cage is formed by a distorted structure adopted by the phosphate binding P-loop and by the activation loop of c-Abl. The P-loop, comprised of the first two β-strands of the N-lobe and the loop connecting them, is normally in an extended conformation. In the STI-571 complex (and in the complex with PD173955; see below) the loop adopts a compact structure that moves Tyr-253 over into close contact with the inhibitor. The hydrophobic cage is completed by resides Leu-370 and Phe-382. A similar hydrophobic cage has been seen previously in the structure of the fibroblast growth factor receptor bound to an inhibitor (22).

The structure of the AblK:STI-571 complex is essentially the same as the structure of AblK:STI-571 (variant). The "left" half of the compound overlaps almost exactly but tilts slightly relative to the variant, beginning at the rightmost phenyl ring (Fig. 4*A*, *left*). The piperazinyl ring (not present in the variant) lies along a partially hydrophobic pocket on the surface, making van der Waals interactions with Val-289, Phe-359, and Asp-381 and hydrogen bonds with the carbonyl oxygen atoms of Ile-360 and His-361. The presence of the piperazinyl ring does not change the conformation of the activation loop, and the mechanism of STI-571 inhibition derived from the AblK:STI-571 (variant) structure remains unchanged.

The kinase domain of c-Abl is about 47% identical in sequence to that of the Src family of tyrosine kinases. Src kinases cannot bind STI-571, even though most of the residues that make contact with the drug in c-Abl are conserved in Src kinases (4). One explanation for this may be due to the differences observed in the inactive conformations of Src and Abl (Fig. 2). It is possible that the activation loop of Src cannot adopt the conformation seen in inactive Abl, although why this is so is unclear. In both Src and Abl, the unphosphorylated

activation loop positions the site of activating tyrosine phosphorylation (Tyr-416 in Src and Tyr-393 in Abl) such that the tyrosine side chain points into the active site, blocking it. The difference is that in the c-Abl structure, the central portion of the activation loop closely mimics the binding of a peptide substrate to the kinase, whereas in Src kinases, it does not.

The conformation of the activation loop in Abl, including the peptide substrate-mimicking element, in general terms resembles the activation loop of unphosphorylated IRK (23). Despite this similarity IRK is not able to bind STI-571 (4). A simple explanation for this is that Thr-315, which makes an important hydrogen bond with STI-571 in the c-Abl complex, is replaced by a bulkier methionine residue in IRK, which would occlude the STI-571 binding site. STI-571 binding is also prevented by a number of subtle differences in the positions of key residues in IRK that are likely to prevent the accommodation of STI-571. For example, Phe-1151 of the DFG motif in inactive IRK completely overlaps the pyrimidine ring of STI-571. Additionally, there are clashes between the piperazinyl ring and Phe-1128 of the catalytic loop. Finally, the conformations of the P-loops in IRK and Abl are quite distinct, and this causes Lys-1030 of IRK to collide with the compound.

Structure of Abl Kinase Domain Bound to PD173955. PD173955 is based on the pyrido-[2,3-d]pyrimidine series of compounds, where the name refers to the central bicyclic ring of the compound (Fig. 1*b*). PD173955 has two substituents, a thiomethyl anilino on the left and a dichlorophenyl on the right, with reference to the orientation in Fig. 1*b*. PD173955 binds between the N- and C-lobes of the kinase domain. It is, however, a smaller molecule than STI-571 and does not reach as deeply into the kinase domain (Fig. 3*A*, *right* and Fig. 4*A*, *right*). The pyrido-pyrimidine ring occupies the place of the pyrimidine and pyridine rings of STI-571, with the additional phenyl and thiomethyl extending outward to solvent. The dichlorophenyl ring occupies a similar position to the core phenyl ring of STI-571. Both compounds have this overlapping phenyl ring rotated such that the plane of the ring is perpendicular to the preceding parts of the compounds. The majority of the interactions between PD173955 and the protein are also mediated by van der Waals interactions (Fig. 3*B*, *right*). Met-318, which hydrogen bonds to STI-571, also hydrogen bonds to PD173955, again through backbone interactions. These are the only hydrogen bonds that PD173955 makes with the protein. Thr-315, which makes an important hydrogen bond with STI-571, only makes van der Waals interactions with PD173955. The two chlorine atoms on the phenyl ring of PD173955 are buried inside the protein, making several van der Waals interactions with Val-256, Ala-269, and Ala-381. The thiomethyl on the other end of the compound is solvent exposed. A total of 913 $Å^2$ of surface area on the inhibitor is buried in the complex.

Conformation of Abl Kinase Domain in Complex with PD173955. The overall conformation of the kinase domain, including the interlobe orientation and the conformation of helix αC, is essentially identical in the STI-571 and PD173955 complexes. However, as noted earlier, the conformations of the activation loops are dramatically different (Figs. 3*A* and 4*B*). Whereas in the AblK:STI-571 structure, this loop is folded in toward the protein (closed) and mimics substrate binding, in the AblK:PD173955 structure, the loop protrudes outward in an extended conformation (open) and resembles that of an activated kinase (20). Beginning at the highly conserved Asp-Phe-Gly (DFG) motif, the loops of AblK:STI-571 and AblK:PD173955 diverge. Asp-381 of AblK:STI-571 continues inward toward the protein, whereas in AblK:PD173955, it extends away from the protein. The loops then meet again at Pro-402.

Although the open conformation of the activation loop seen here resembles that seen in the structure of active kinases such as Lck, the DFG motifs are quite different (Fig. 4*B*, *middle* and *right*). Again, beginning at Asp-381 (Asp-382 in Lck), the residues kink in opposite directions such that Phe-383 in Lck occupies the space of Asp-381 in AblK:PD173955 and *vice versa*. Following this, the loops follow essentially the same path. The sites of phosphorylation in the activation loops, Tyr-393 in Abl and Tyr-394 in Lck, have essentially the same conformation. In Lck, Tyr-394 is phosphorylated and makes critical hydrogen bonds with the side chain of Arg-387, which presumably stabilizes the open conformation. In Ablk:PD173955, Tyr-393 is not phosphorylated and does not make any hydrogen bonds. Arg-386 (equivalent to Arg-387 in Lck) has weak electron density, points into the solvent, and does not contribute to the stabilization of the open conformation. This suggests that the c-Abl kinase domain, at least in isolation, can achieve the open conformation in the absence of phosphorylation, although in solution this conformation is probably short-lived relative to a Tyr-393-phosphorylated state due to the lack of ionic stabilizing interactions between phosphorylated Tyr-393 and Arg-386.

Differences between the Recognition of STI-571 and PD173955 by Abl Kinase. Although STI-571 and PD173955 bind to essentially the same site in Abl kinase, the difference in size of the compounds imparts differences in binding characteristics. Interestingly, a total of 21 protein residues interact with STI-571, compared to only 11 residues with PD173955 (Fig. 3*B*), yet PD173955 is found to be significantly more inhibitory. Thus, the extent of the binding interface (1251 $Å^2$ for STI-571 and 913 $Å^2$ for PD173955), which is often correlated with binding energy, cannot explain the greater potency of PD173955.

To reconcile this, we modeled PD173955 and STI-571 into both the open and closed conformations of Abl. The model of PD173955 in the structure of the inactive conformation of Abl reveals that it can nestle into the binding pocket without any major clashes with protein atoms (Fig. 5*A*), although minor adjustments of the P-loop are necessary. This loop is known to be highly flexible in kinases due to its high glycine content. As suggested in the AblK:STI-571 (variant) structure, the conformation of the P-loop is likely induced by the presence of the inhibitor. In this case, a small shift in the position of Tyr-253 is required to accommodate the additional sulfur-containing phenyl group of PD173955, which faces solvent.

In marked contrast, STI-571 cannot be accommodated in the form of Abl that PD173955 recognizes (Fig. 5*B*). Beyond the secondary amino group of STI-571, both the phenyl ring and piperazinyl ring collide with residues of the activation loop in the open conformation, most notably Asp-381 and Leu-384. Thus, PD173955 can probably bind to Abl regardless of the conformation of the activation loop, whereas STI-571 requires that the activation loop be in the observed closed conformation. Once STI-571 is bound to Abl, it jams between the activation loop and helix αC, preventing the activation loop from changing conformation. For the PD173955 compound, the smaller size of the compound prevents the activation loop from being jammed. The fact that only the open conformation of the activation loop is observed in the structure of Ablk:PD173955 is perhaps a consequence of the requirements for crystal lattice formation. In solution, the isolated kinase domain of Abl probably exists in dynamic equilibrium between open and closed conformations of the activation loop.

To test whether PD173955 is sensitive to activation loop phosphorylation, we performed a kinase inhibition assay with varying concentrations of PD173955 and STI-571, using both phosphorylated and unphosphorylated forms of the kinase domain of Abl. We have previously shown that STI-571 is an effective inhibitor only when the kinase is unphosphorylated (6). Based on the above modeling, we expect PD173955 to be insensitive to the phosphorylation state of Abl. Our results indicate that this is indeed the case. In the presence of

STI-571, pAbl displays significant levels of kinase activity (*i.e.*, STI-571 is only weakly inhibitory). Only upon dephosphorylation of Abl does STI-571 display significant inhibitory action (Fig. 6*A*), as seen previously (6). In contrast, the inhibition profile of PD173955 shows that the drug is effective against Abl regardless of its phosphorylation state (Fig. 6*B*). Furthermore, based on the inhibition curves, it was found that PD173955 is much more potent than STI-571, inhibiting Abl with an IC_{50} of about 5 nM (independent of the phosphorylation state), whereas STI-571 inhibits Abl at approximately 100 nM (dephosphorylated Abl only). This suggests that although PD173955 makes fewer contacts with Abl, it inhibits more potently because it can recognize multiple forms of the kinase. STI-571, on the other hand, requires a specific conformation of the kinase before it can bind. A portion of the binding free energy of STI-571 to Abl may be used to stabilize an otherwise flexible unphosphorylated activation loop, resulting in a less-than-expected observed affinity. With PD173955, only the ATP-binding pocket is obscured, and the activation loop likely remains flexible in the presence of the drug. If it were possible to isolate the Abl kinase domain in only the observed closed conformation, one might expect that the affinity of STI-571 for such a "frozen" Abl would likely surpass the affinity of PD173955 for Abl because STI-571 interacts so much more extensively with the kinase.

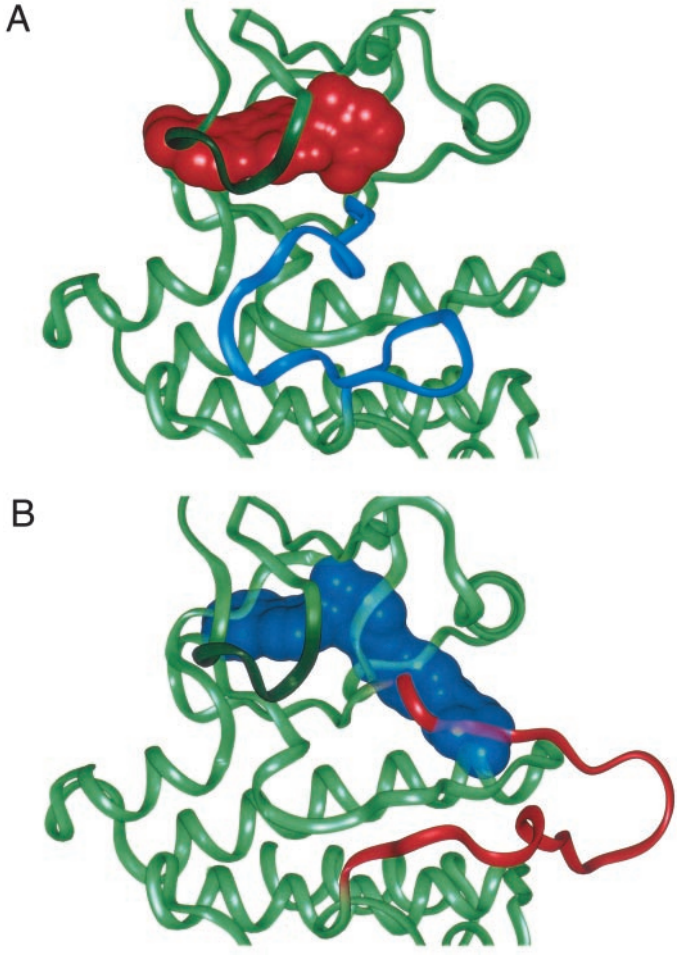

Fig. 5. *A*, PD173955 shown as a van der Waals surface (*red*) modeled into the Abl kinase domain (*green*) conformation that binds to STI-571. No major clashes occur with the activation loop (*blue*) or any other parts of the protein. *B*, van der Waals representation of STI-571 (*blue*) in the conformation of Abl kinase (*green*) that crystallized with PD173955. In this case, major clashes occur with STI-571 and the activation loop (*red*). The P-loop is shown in *dark green* in both *A* and *B*.

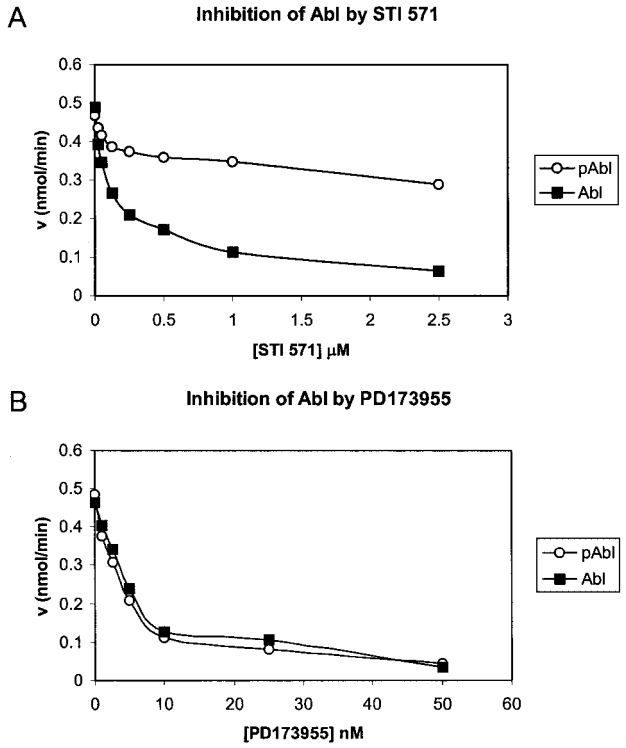

Fig. 6. Effects of STI-571 (*A*) and PD173955 (*B*) on Abl catalyzed phosphorylation. The dose response of pAbl is shown with *empty circles*, and that of dephosphorylated Abl is shown with *filled squares*. The reaction rates are corrected for the rate of a control reaction in the absence of peptide substrate. The amount of Src used did not give a significant signal in the spectrophotometric assay.

Phosphorylation Switch of the Abl Kinase Domain. In CML cells, c-Abl is fused with Bcr, causing it to be constitutively active. Thus, the activation loop in Bcr-Abl would, for the most part, be phosphorylated and in the open conformation. Given that STI-571 cannot recognize this open conformation, how then does STI-571 achieve its great inhibitory effect? One possibility is that the phosphorylation state of the activation loop is dynamic. The action of cellular phosphatases constantly counteracts the kinase activity of the Bcr-Abl complex, and when the activation loop is transiently dephosphorylated, STI-571 can bind and inactivate the kinase. Another possibility is that STI-571 traps newly synthesized Bcr-Abl and shuts off its phosphorylation capability early on. PD173955, on the other hand, can probably inhibit Bcr-Abl regardless of the phosphorylation state it is in.

It is hoped that by understanding how small molecule inhibitors such as STI-571 and PD173955 exert their influence at the molecular level, we can gain insight into making rational modifications to them in the hopes of producing drugs for improved leukemia therapy.

ACKNOWLEDGMENTS

We thank Huguette Viguet for Sf9 cell culture. Figures were generated using Insight II and Setor (25).

REFERENCES

1. Van Etten, R. A. Cycling, stressed-out and nervous: cellular functions of c-Abl. Trends Cell Biol, *9:* 179–186, 1999.
2. Jackson, P., and Baltimore, D. N-terminal mutations activate the leukemogenic potential of the myristoylated form of c-abl. EMBO J., *8:* 449–456, 1989.
3. Pendergast, A. M., Gishizky, M. L., Havlik, M. H., and Witte, O. N. SH1 domain autophosphorylation of P210 BCR/ABL is required for transformation but not growth factor independence. Mol. Cell. Biol., *13:* 1728–1736, 1993.

4. Druker, B. J., Tamura, S., Buchdunger, E., Ohno, S., Segal, G. M., Fanning, S., Zimmermann, J., and Lydon, N. B. Effects of a selective inhibitor of the Abl tyrosine kinase on the growth of Bcr-Abl positive cells. Nat. Med., *2:* 561–566, 1996.
5. Kantarjian, H., Sawyers, C., Hochhaus, A., Guilhot, F., Schiffer, C., Gambacorti-Passerini, C., Niederwieser, D., Resta, D., Capdeville, R., Zoellner, U., Talpaz, M., and Druker, B. Hematologic and cytogenetic responses to imatinib mesylate in chronic myelogenous leukemia. N. Engl. J. Med., *346:* 645–652, 2002.
6. Schindler, T., Bornmann, W., Pellicena, P., Miller, W. T., Clarkson, B., and Kuriyan, J. Structural mechanism for STI-571 inhibition of abelson tyrosine kinase. Science (Wash. DC), *289:* 1938–1942, 2000.
7. Dorsey, J. F., Jove, R., Kraker, A. J., and Wu, J. The pyrido[2,3-d]pyrimidine derivative PD180970 inhibits p210Bcr-Abl tyrosine kinase and induces apoptosis of K562 leukemic cells. Cancer Res., *60:* 3127–3131, 2000.
8. Moasser, M. M., Srethapakdi, M., Sachar, K. S., Kraker, A. J., and Rosen, N. Inhibition of Src kinases by a selective tyrosine kinase inhibitor causes mitotic arrest. Cancer Res., *59:* 6145–6152, 1999.
9. Wisniewski, D., Lambek, C.L. , Liu, C., Strife, A., Veach, D. R., Nagar, B., Young, M. A., Schindler, T., Bornmann, W. G., Bertino, J. R., Kuriyan, J., and Clarkson, B. Characterization of potent inhibitors of the Bcr-Abl and the c-Kit receptor tyrosine kinases. Cancer Res., *62:* 4244–4255, 2002.
10. Zimmermann, J., Buchdunger, E., Mett, H., Meyer, T., and Lydon, N. B. Potent and selective inhibitors of the Abl-kinase: phenylamino-pyrimidine (PAP) derivatives. Bioorg. Med. Chem. Lett., *7:* 187–192, 1997.
11. Kraker, A. J., Hartl, B. G., Amar, A. M., Barvian, M. R., Showalter, H. D., and Moore, C. W. Biochemical and cellular effects of c-Src kinase-selective pyrido[2,3-d]pyrimidine tyrosine kinase inhibitors. Biochem. Pharmacol., *60:* 885–898, 2000.
12. Otwinowski, Z., and Minor, W. Processing of X-ray diffraction data collected in oscillation mode. Methods Enzymol., *276:* 307–326, 1997.
13. Navaza, J. AMoRe: an automated package for molecular replacement. Acta Crystallogr. Sect. A Foundations of Crystallography, *50:* 157–163, 1994.
14. Brunger, A. T., Adams, P. D., Clore, G. M., DeLano, W. L., Gros, P., Grosse-Kunstleve, R. W., Jiang, J. S., Kuszewski, J., Nilges, M., Pannu, N. S., Read, R. J., Rice, L. M., Simonson, T., and Warren, G. L. Crystallography & NMR system: a new software suite for macromolecular structure determination. Acta Crystallogr. Sect. D Biol. Crystallogr., *54* (Pt 5)*:* 905–921, 1998.
15. Jones, T. A., Zou, J. Y., Cowan, S. W., and Kjeldgaard Improved methods for binding protein models in electron density maps and the location of errors in these models. Acta Crystallogr. Sect. A Foundations of Crystallography, *47:* 110–119, 1991.
16. Barker, S. C., Kassel, D. B., Weigl, D., Huang, X., Luther, M. A., and Knight, W. B. Characterization of pp60c-src tyrosine kinase activities using a continuous assay: autoactivation of the enzyme is an intermolecular autophosphorylation process. Biochemistry, *34:* 14843–14851, 1995.
17. Warmuth, M., Bergmann, M., Priess, A., Hauslmann, K., Emmerich, B., and Hallek, M. The Src family kinase Hck interacts with Bcr-Abl by a kinase-independent mechanism and phosphorylates the Grb2-binding site of Bcr. J. Biol. Chem., *272:* 33260–33270, 1997.
18. Plattner, R., Kadlec, L., DeMali, K. A., Kazlauskas, A., and Pendergast, A. M. c-Abl is activated by growth factors and Src family kinases and has a role in the cellular response to PDGF. Genes Dev., *13:* 2400–2411, 1999.
19. Knighton, D. R., Zheng, J. H., Ten Eyck, L. F., Ashford, V. A., Xuong, N. H., Taylor, S. S., and Sowadski, J. M. Crystal structure of the catalytic subunit of cyclic adenosine monophosphate-dependent protein kinase. Science (Wash. DC), *253:* 407–414, 1991.
20. Yamaguchi, H., and Hendrickson, W. A. Structural basis for activation of human lymphocyte kinase Lck upon tyrosine phosphorylation. Nature (Lond.), *384:* 484–489, 1996.
21. Zheng, J., Knighton, D. R., ten Eyck, L. F., Karlsson, R., Xuong, N., Taylor, S. S., and Sowadski, J. M. Crystal structure of the catalytic subunit of cAMP-dependent protein kinase complexed with MgATP and peptide inhibitor. Biochemistry, *32:* 2154–2161, 1993.
22. Mohammadi, M., McMahon, G., Sun, L., Tang, C., Hirth, P., Yeh, B. K., Hubbard, S. R., and Schlessinger, J. Structures of the tyrosine kinase domain of fibroblast growth factor receptor in complex with inhibitors. Science (Wash. DC), *276:* 955–960, 1997.
23. Hubbard, S. R., Wei, L., Ellis, L., and Hendrickson, W. A. Crystal structure of the tyrosine kinase domain of the human insulin receptor. Nature (Lond.), *372:* 746–754, 1994.
24. Schindler, T., Sicheri, F., Pico, A., Gazit, A., Levitzki, A., and Kuriyan, J. Crystal structure of Hck in complex with a Src family-selective tyrosine kinase inhibitor. Mol. Cell, *3:* 639–648, 1999.
25. Evans, S. V. SETOR: Hardware-lighted three-dimensional solid model representations of macromolecules. J. Mol. Graph, *11:* 134–138, 1993.